Investigation of Statistical Inference Methodologies Through Scale Model Propagation Experiments

Jason D. Sagers
Applied Research Laboratories at The University of Texas at Austin
Environmental Science Laboratory
Austin, TX 78758
phone: (512) 835-3195 fax: (512) 490-4225 email: sagers@arlut.utexas.edu

Award Number: N00014-15-1-2017

LONG-TERM GOALS

The long-term scientific goal of this project is to advance the understanding of statistical inference methodologies for ocean-acoustic problems by investigating and applying statistical methods to data collected from scale-model propagation experiments.

OBJECTIVES

The scientific objectives for FY2015 were to (1) complete three-dimensional (3D) laboratory propagation experiments over a translationally invariant wedge, (2) to plan and conduct 3D propagation experiments over the Hudson Canyon scale-model bathymetry, and (3) to begin planning experiments for statistical inference applications.

APPROACH

In the ocean acoustics community over the past two decades, statistical inference of ocean waveguide properties [1–5] has effectively replaced matched-field and inversion type approaches.[6] This change in perspective is based on the realization that the multi-parameter inverse problem for ocean waveguides is non-unique, resulting in many possible good solutions and no consistent way to discriminate between them. Consequently, a probabilistic description is needed to assign meaning to the set of possible solutions for waveguide parameters.

With the introduction of statistical inference to the field of ocean acoustics came the desire to interpret marginal probability distributions as the statistical distributions of real waveguide parameters. This is recognized in the literature when authors compare an inferred marginal distribution to an independent measurement of the physical parameter, which is called ground truthing (cf. Refs. 2; 3; 5; 7–10). Nearly all of the published papers on the statistical inference of data collected at-sea that assign meaning to inferred marginal distributions utilize the ground-truth approach. It is obviously desirable to interpret probability distributions inferred from acoustic measurements as statistical distributions of physical waveguide parameters, but it may not always be appropriate to do so. One reason is that the true

Green's function which exists in the ocean for a given space and time can never be exactly described by an effective Green's function generated by an acoustic propagation model. The difference between the true and modeled Green's functions can be termed model error and can affect the interpretation of the inference result.

The approach taken in this work is to apply statistical inference methodologies to data collected from well-controlled laboratory acoustic propagation experiments, and then to investigate the important concepts of ground truthing, model error, and the ability of the data to resolve inherent ambiguities between waveguide parameters. There are at least two potential advantages to this approach. The first is the ability to accurately prescribe and/or measure waveguide parameters while simultaneously collecting the acoustic data, which could give more meaning and context to the ground truthing process. The second is the ability to conduct rapid, systematic, and relatively inexpensive experiments to explore issues related to the application of statistical inference methods to acoustic propagation data.

The indoor tank facility where the measurements are made resides at the Applied Research Laboratories at The University of Texas at Austin (ARL:UT). A detailed description of the measurement apparatus along measurement examples are found in Refs. 11–13.

WORK COMPLETED

The work completed during FY15 includes the two experiments listed below. Results in each of these areas are discussed in the next section.

1. *Completion of an acoustic propagation experiment over a translationally invariant wedge.* The purpose of this experiment was to continue the verification process of the apparatus, and to observe modal shadow zones and multi-mode interference by direct measurement. It is anticipated that the data collected from this experiment can be used to infer information about the source/receiver geometry, bathymetry, and the strength of acoustic mode coupling.
2. *Completion of an acoustic propagation experiment over the Hudson Canyon bathymetry.* The purpose of this experiment was to observe the complicated three-dimensional propagation effects over a non-ideal sloping bathymetry. It is anticipated that the data collected from this experiment can be used to asses how the inference of certain parameter values could be affected by model error.

RESULTS

1. Translationally invariant wedge propagation experiments

The layout of the source and receiver geometry relative to a wedge of 10° slope is shown in Fig. 1. The wedge is made from closed cell polyurethane foam and approximates a pressure release boundary. The apex of the wedge intersects the air/water interface along the line Y = 109.2 cm. The source was located on the wedge at (X, Y, Z) = (188, 86.4, 2.0) cm and a total of 1,310 synthetic vertical line arrays (VLAs) were located between X = 12.7 and X = 177.8 cm and between Y = 86.4 and Y = 97.8 cm at 1.3 cm spacing. The acoustic field was measured in the vertical dimension by the receiving transducer at each VLA location, from approximately 6.4 mm above the bottom up to the air/water interface at a spacing of 1.3 mm. The data acquisition at each measurement point was triggered so that precise time alignment was possible during post-processing.

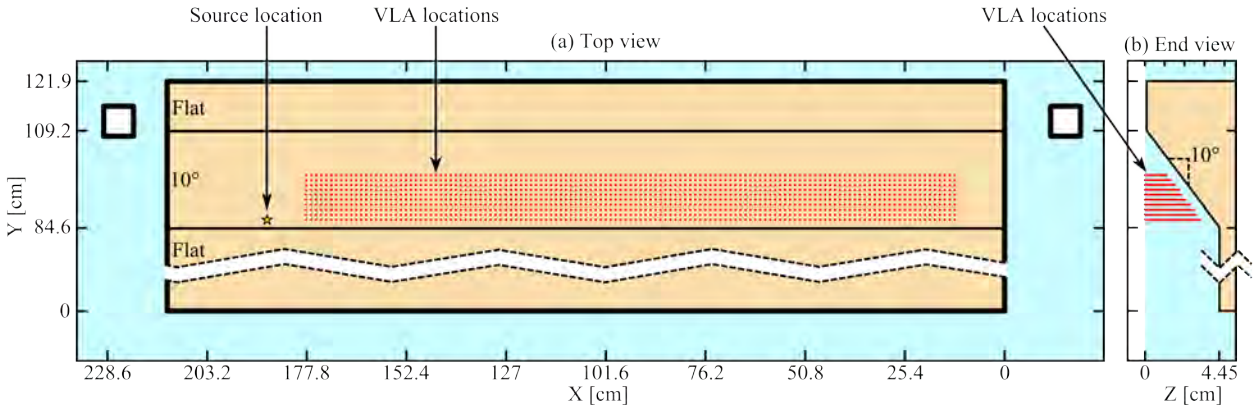

Figure 1: (a) Top and (b) end views showing the source location and VLA measurement locations on the 10° wedge.

This particular experimental geometry gives rise to 3D acoustic propagation, which can be described by a set of horizontal rays for each vertical mode.[14] For illustration, a portion of a calculated horizontal ray set for modes 1, 3, 5, and 7 at 300 kHz are shown in Fig. 2 superimposed on the grid of VLA locations. Each time the acoustic wavefront interacts with the wedge, it is reflected by the sloped bottom toward deeper water, causing a curved, or "horizontally refracted," ray trace in the horizontal plane. For each mode there is a limiting ray which bounds the region where acoustic energy can propagate in that mode. The region where the acoustic energy does not propagate is called a modal shadow zone.[15] This

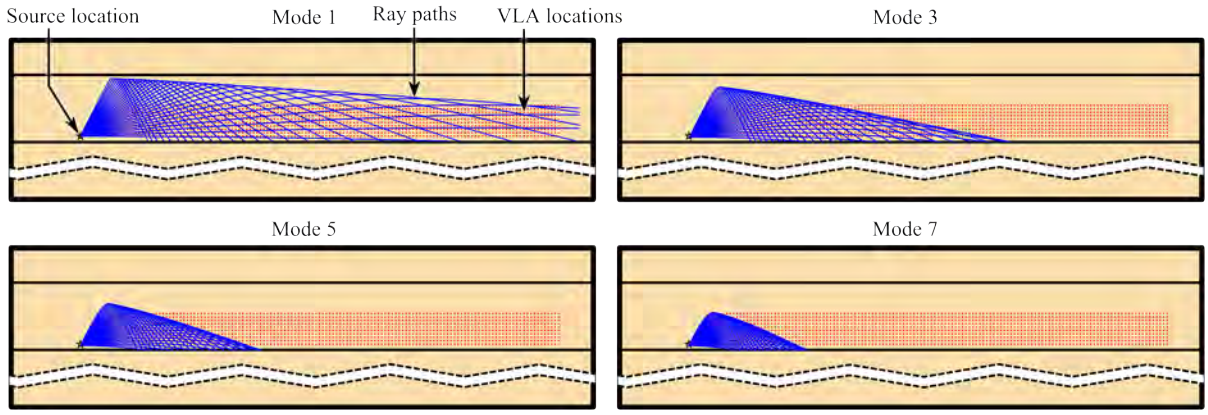

Figure 2: Horizontal ray paths for modes 1, 3, 5, and 7 at 300 kHz superimposed on the grid of VLA measurement locations.

phenomenon has been previously observed by Sturm and Korakas in laboratory measurements for a small number of measurement locations over a sand wedge.[16] The measurement described here seeks to expand upon the previous work by collecting enough data to perform modal decomposition of the acoustic field at multiple points in the horizontal plane, and thus to directly observe the modal shadow zones through a plot of mode amplitudes.

At each VLA location and for each mode there are exactly two horizontal ray paths between the source and receiver. The first ray propagates at a shallower horizontal angle relative to the X-axis, while the

second ray takes a steeper horizontal angle, propagates farther up the wedge, resulting in a longer ray path length than the first ray. Depending on the range to the receiver, the acoustic energy in the two ray paths can arrive with variable relative phasing, giving rise to intramode interference.[17] It is possible that the details of the intramode interference are sensitive to both geometric and waveguide parameters and that these patterns could be used in an inference approach. Future work will investigate this possibility.

The source signal was a pulsed waveform containing 100 cycles of a 300 kHz sine wave. Amplitude shading in the form of a Tukey window with $\alpha = 0.05$ was applied to taper the edges of the waveform. The source transducer was located at one-half of the waveguide depth for the purpose of only exciting the odd-numbered modes, although the finite size of the transducer element will impact the modal excitation. The measured acoustic data for this experiment are shown on a reduced time scale, $t_{reduced} = t - dc$, where d is the distance between the source and receiver and c is the water sound speed. The water layer in the laboratory tank is isospeed with $c = 1480$ m/s.

Figures 3(a) and (b) respectively show the acoustic intensity in each of 10 XZ planes and the filtered normal mode amplitudes in the XY plane at $t_{reduced} = 15\mu$s. The modal shadow zones are clearly seen in Fig. 3(b), and can also be identified in (a) by the stripping of higher-order modes from the interference pattern as a function of X and Y position. This particular time was selected for display because the acoustic energy from the second ray path had not yet arrived at the receiver locations and therefore intramode interference was absent. Figures 3(c) and (d) display the data at $t_{reduced} = 150\mu$s, when the second ray has arrived at the receivers and steady-state conditions were established. The intramode interference is manifest by the additional interference pattern in the acoustic intensity and in the striated normal mode amplitudes across the horizontal plane.

2. Hudson Canyon propagation experiments

Both along-axis and across-axis propagation experiments were conducted over a bathymetry which was specially fabricated as a scale-model representation of a portion of the Hudson Canyon. The source waveform for both experiments consisted of a 50 μs long LFM chirp with a center frequency of 1 MHz and a bandwidth of 2 MHz. For the along-axis experiment, the source transducer was located at (X, Y, Z) = (188, 61, 6.7) cm and acoustic data were measured in 1) the XY plane at Z = 2.5 mm, 2) the XZ plane at Y = 61 cm, and 3) at three 10.2 cm long horizontal line arrays (HLAs) located in the middle of the water column at X-coordinates of 127, 76.2, and 25.4 cm. Figures 4(a) and (b) show top and side views, respectively, of the bathymetry with the measurement locations superimposed. Figure 4(a) is also superimposed with the acoustic intensity (color data) measured in the XY plane at a time of 375 μs, just prior to the direct-path wavefront arriving at the first HLA. The acoustic data show that the bottom-interacting wavefronts (those to the left of the cylindircally expanding direct-path wavefront) have already undergone horizontal refraction from the canyon walls. Horizontal refraction is also visible in the beamformed data from HLAs 1 through 3, shown in Fig. 4(c) through (e), respectively. At the first HLA position, the direct-path wavefront arrives near 400 μs and 0°, immediately followed by a string of additional wavefronts with positive arrival angles relative to broadside. The first strong arrival at negative array angles occurs near 600 μs. This is not unexpected, as the Y = 61 cm plane is slightly closer to one canyon wall than the other near the source position. The canyon produces a focusing effect on the acoustic propagation, which is visible in Figs. 4(c) through (e) by the reduction in the angular spread of the arriving energy with increasing HLA range from the source.

For the across-axis propagation experiment, the source transducer was located at (X, Y, Z) = (106.7, 10.2, 1.4) cm and acoustic data were measured in 1) the YZ plane at X = 106.7 cm, and 2) at two

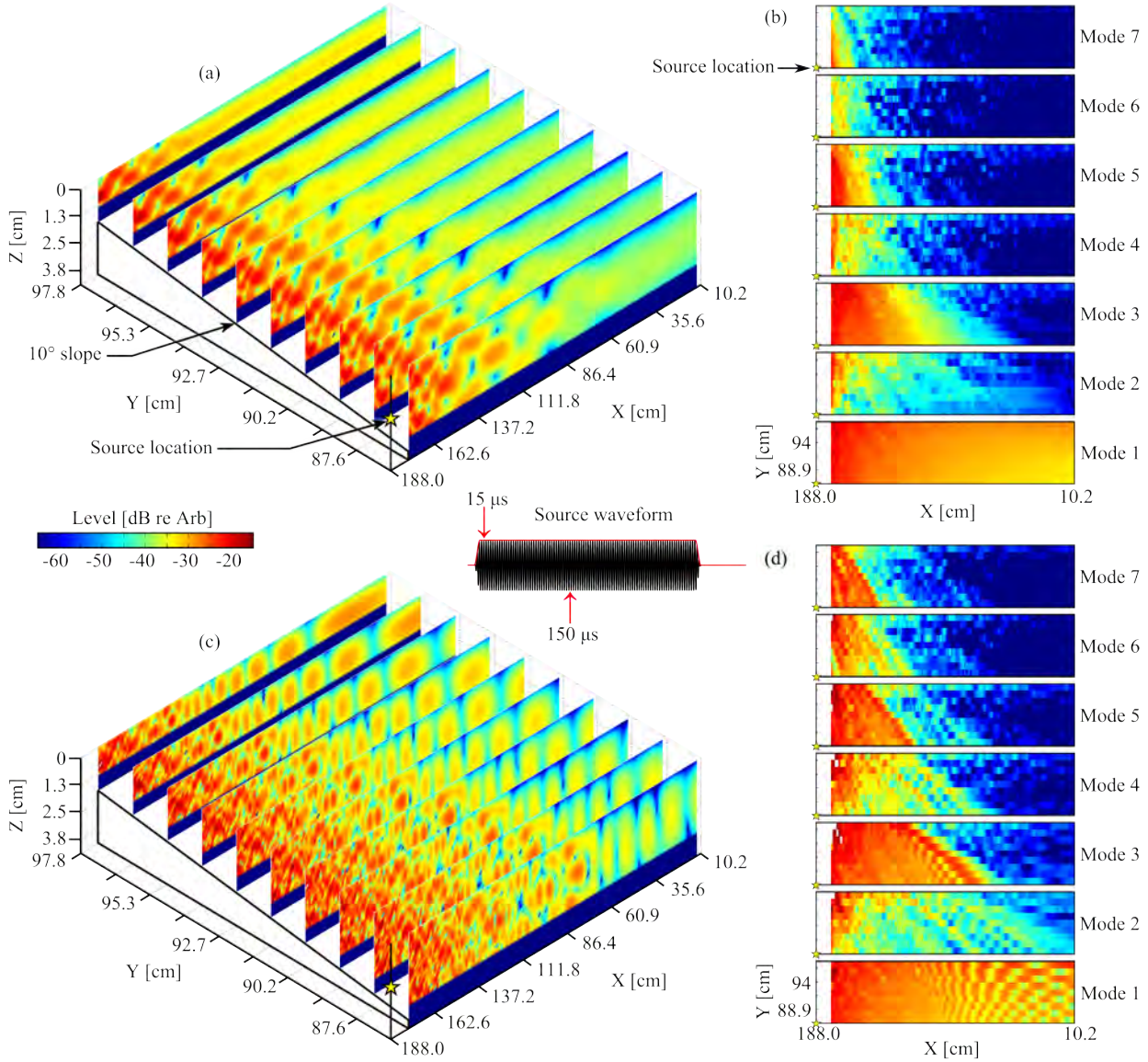

Figure 3: (a) Measured acoustic intensity in 10 XZ planes on the wedge and (b) filtered normal mode amplitudes displayed in the XY plane at $t_{reduced} = 15\mu s$. Subplots (c) and (d) are the same as (a) and (b), respectively, except at $t_{reduced} = 150\mu s$. The amplitude shaded source waveform is displayed in the center of the figure for reference.

10.2 cm long HLAs located in the middle of the water column at Y-coordinates of 63.5 and 101.6 cm. Figures 5(a) through (d) show side views of the bathymetry in the measurement plane and HLA locations with acoustic intensity (color data) superimposed at t = 350, 650, 800, and 1200 μs, respectively. In Fig. 5(a) all of the energy is propagating from left to right and is marked above the figure with a bracket and the number 0, indicating that this packet of energy has not undergone a reversal of propagation direction. The corresponding energy is also visible in the beamformed data of Figs. 5(e) and (f) and arrives near 0° relative to broadside. Figure 5(b) shows the initial packet of energy as it has propagated farther to the right and also gives the first indication of backscattered energy, marked with the number 1 above the figure. The backscattered energy becomes much more visible in Fig. 5(c) as it gains spatial separation from the initial packet. The backscattered energy is also visible in

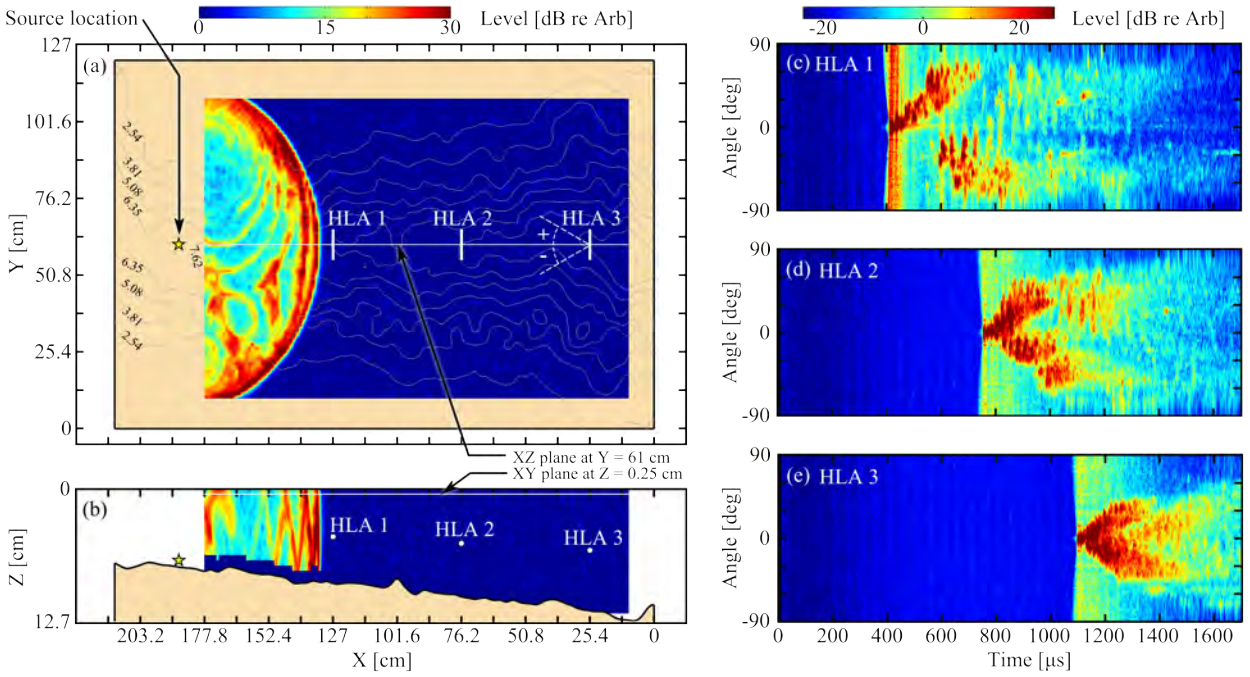

Figure 4: (a) Top view of the Hudson Canyon bathymetry contours (gray lines, labeled in cm) superimposed with three HLA measurement locations and measured acoustic data in the XY plane at Z = 2.5 mm (color data) at $t = 375\mu$s. (b) Side view of the XZ plane at Y = 61 cm. Subplots (c) through (e) show beamformed data on the three HLAs.

Fig. 5(e) between t = 600 μs and 1100 μs. It appears that this energy passes the first HLA at three discrete horizontal angles, which may suggest regions of the bathymetry which preferentially scattered energy back toward the array. Finally, Fig. 5(d) shows the first backscattered packet of energy as it has propagated farther to the left and scatters another packet of energy back to the right. Because of the low signal amplitude of the second backscattering event, this energy is more clearly visible in Fig. 5(e) between t = 1200 μs and 1500 μs. Future work will focus on applying a 3D numerical model and comparing the measured and modeled data. From there, an inference process with an emphasis on finding and quantifying the sources of model error could be completed.

IMPACT/APPLICATIONS

The impact of this research is to understand the the issues associated with applying statistical inference methodologies to underwater acoustic data.

RELATED PROJECTS

None

REFERENCES

[1] P. Gerstoft and C. F. Mecklenbruker, "Ocean acoustic inversion with estimation of a posteriori probability distributions," J. Acoust. Soc. Am. **104**, 808–819 (1998).

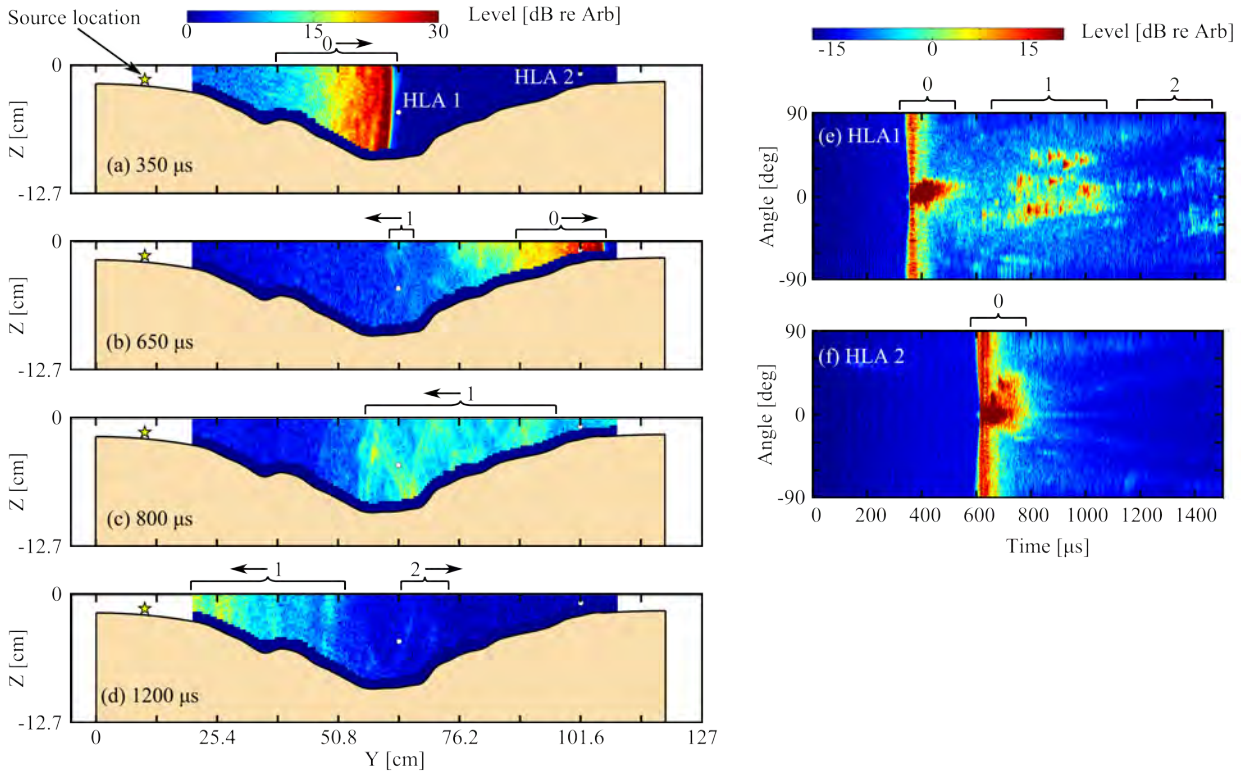

Figure 5: Subplots (a) through (d) show measured acoustic data in the YZ plane at X = 107 cm for the across-axis experiment at various time samples, with HLA positions (white dots) superimposed. Subplots (e) and (f) show beamformed acoustic data on the two HLAs. The initial forward propagating energy is marked with a 0 above the plots, and the two backscattering events are marked with 1 and 2.

[2] S. E. Dosso, "Quantifying uncertainty in geoacoustic inversion. I. a fast Gibbs sampler approach," J. Acoust. Soc. Am. **111**, 129–142 (2002).

[3] S. E. Dosso and P. L. Nielsen, "Quantifying uncertainty in geoacoustic inversion. II. application to broadband, shallow-water data," J. Acoust. Soc. Am. **111**, 143–159 (2002).

[4] M. K. Sen and P. L. Stoffa, "Bayesian inference, Gibbs' sampler, and uncertainty estimation in geophysical inversion," Geophys. Prospect. **44**, 313–350 (1996).

[5] D. P. Knobles, J. D. Sagers, and R. A. Koch, "Maximum entropy approach to statistical inference for an ocean acoustic waveguide," J. Acoust. Soc. Am. **131**, 1087–1101 (2012).

[6] N. R. Chapman and D. P. Knobles, "Perspectives on geoacoustic inversion," AIP Conference Proceedings **1495**, 202–221 (2012).

[7] C. W. Holland, "Geoacoustic inversion for fine-grained sediments," J. Acoust. Soc. Am. **111**, 1560–1564 (2002).

[8] S. Dosso and M. Wilmut, "Data uncertainty estimation in matched-field geoacoustic inversion," IEEE J. Oceanic Eng. **31**, 470–479 (2006).

[9] Y. M. Jiang, N. R. Chapman, and M. Badiey, "Quantifying the uncertainty of geoacoustic

parameter estimates for the New Jersey shelf by inverting air gun data," J. Acoust. Soc. Am. **121**, 1879–1894 (2007).

[10] J. Bonnel, S. E. Dosso, and N. R. Chapman, "Bayesian geoacoustic inversion of single hydrophone light bulb data using warping dispersion analysis," J. Acoust. Soc. Am. **134**, 120–130 (2013).

[11] J. D. Sagers, "Results from a scale model acoustic propagation experiment over a translationally invariant wedge," Proceedings of Meetings on Acoustics **22** (2015).

[12] J. D. Sagers, "Three-dimensional scale-model tank for model ocean acoustics experiments," ONR DURIP Final Report N00014-13-1-0713, The University of Texas at Austin (2015).

[13] J. D. Sagers, "Three-dimensional acoustic propagation over a translationally invariant wedge and in a scale-model canyon," in *3rd Underwater Acoustics Conference and Exhibition*, edited by J. S. Papadakis and L. Bjorno, 3–12 (2015).

[14] H. Weinberg and R. Burridge, "Horizontal ray theory for ocean acoustics," J. Acoust. Soc. Am. **55**, 63–79 (1974).

[15] C. H. Harrison, "Acoustic shadow zones in the horizontal plane," J. Acoust. Soc. Am. **65**, 56–61 (1979).

[16] F. Sturm and A. Korakas, "Comparisons of laboratory scale measurements of three-dimensional acoustic propagation with solutions by a parabolic equation model," J. Acoust. Soc. Am. **133**, 108–118 (2013).

[17] M. J. Buckingham, "Theory of three-dimensional acoustic propagation in a wedgelike ocean with a penetrable bottom," J. Acoust. Soc. Am. **82**, 198–210 (1987).

PUBLICATIONS

Peer-reviewed papers

J. D. Sagers and M. S. Ballard, "Testing and verification of a scale-model acoustic propagation system," submitted to J. Acoust. Soc. Am., [in review, refereed].

J. D. Sagers, M. S. Ballard, and D. P. Knobles, "Evidence of three-dimensional acoustic propagation in the Catoche Tongue," J. Acoust. Soc. Am., **136**, 2453-2462 (2014) [published, refereed].

Conference presentations/proceedings

J. D. Sagers, "Measurements of three-dimensional acoustic propagation over a translationally invariant wedge and in a scale-model canyon," in proceedings of the 3rd Underwater Acoustics Conference and Exhibition, edited by J. S. Papadakis and L. Bjorno, 3-12 (2015) [UACE presentation and proceedings paper].

J. D. Sagers, "Measurements of three-dimensional acoustic propagation in a scale-model canyon," J. Acoust. Soc. Am., **137**, 2391 (2015) [ASA presentation].

J. D. Sagers, "Results from a scale model acoustic propagation experiment over a translationally invariant wedge," Proc. Mtgs. on Acoust., **22**, 070001 (2015) [published, reviewed].

M. S. Ballard and J. D. Sagers, "Numerical modeling of measurements from an underwater scale-model tank experiment," J. Acoust. Soc. Am., **136**, 2178 (2014) [ASA presentation].

M Badiey, A. Muenchow, L. Wan, M. S. Ballard, D. P. Knobles, and J. D. Sagers, "Modeling three dimensional environment and broadband acoustic propagation in the Arctic shelf-basin region," J. Acoust. Soc. Am., **136**, 2317 (2014) [ASA presentation].